

Protein Microarrays for the Identification of Praja1 E3 Ubiquitin Ligase Substrates

Christian M. Loch · Michael J. Eddins ·
James E. Strickler

Published online: 2 April 2011
© Springer Science+Business Media, LLC 2011

Abstract Although they are the primary determinants of substrate specificity, few E3-substrate pairs have been positively identified, and few E3's profiled in a proteomic fashion. Praja1 is an E3 implicated in bone development and highly expressed in brain. Although it has been well studied relative to the majority of E3's, little is known concerning the repertoire of proteins it ubiquitylates. We sought to identify high confidence substrates for Praja1 from an unbiased proteomic profile of thousands of human proteins using protein microarrays. We first profiled Praja1 activity against a panel of E2's to identify its optimal partner *in vitro*. We then ubiquitylated multiple, identical protein arrays and detected putative substrates with reagents that vary in ubiquitin recognition according to the extent of chain formation. Gene ontology clustering identified putative substrates consistent with information previously known about Praja1 function, and provides clues into novel aspects of this enzyme's function.

Keywords Ubiquitin · Ligase · Microarray · Praja1

Introduction

At over 600 members, the E3 ubiquitin ligases constitute the largest family of enzymes in the human proteome [1]. Working in concert with two E1 ubiquitin activating

enzymes and an unique subset of the roughly 30 human E2 ubiquitin conjugating enzymes [2], it is the responsibility of the E3's to transfer ubiquitin to the epsilon amine of lysine in target protein substrates. Along with the roughly 100 deubiquitylase enzymes [DUBs; 3, 4], it is their charge to make sure that this conjugation is done with temporal and spatial specificity, to only the intended lysines on specified proteins, with the appropriate number of ubiquitin moieties chain-linked to said lysine(s) (where $n = 1$ termed monoubiquitylation and where $n \geq 2$ polyubiquitylation), and finally that the linkages and branch points between and among individual ubiquitin moieties of the chain (polyubiquitylation only) is correct for the intended consequence to the target protein. Once dismissed as a "simple" tag for the "garbage can of the cell" i.e., the proteasome, ubiquitin signaling is now appreciated to have consequences for protein localization, protein function, protein-protein interaction, and (yes) protein degradation [5–12]. Failure in this system at almost any step just mentioned has the potential to result in improper protein homeostasis for the roughly 90% of cellular proteins it regulates [13], which in turn has potential to result in any number of human pathologies driven at the protein level like infection and immune response [14, 15], cystic fibrosis [16], muscle control and wasting [17], cardiovascular diseases [18], neurodegeneration [19], and cancer [20], to name a few. The complexity of the system and its near-ubiquitous importance to human health suggests that its increasing profile as a diagnostic and therapeutic target is a trend unlikely to reverse let alone slow down any time soon.

Praja1 is an E3 ubiquitin ligase implicated in bone and liver development as well as memory formation and X-linked mental retardation [21–24]. Transcript has been localized in brain, liver, kidney, and embryo [22]; expression has been seen in wound healing [23], brain [24], and in

C. M. Loch (✉) · J. E. Strickler
Division of Research & Development, LifeSensors, Inc,
271 Great Valley Parkway, Malvern, PA 19355, USA
e-mail: loch@lifesensors.com

M. J. Eddins
Progenra, Inc, 277 Great Valley Parkway, Malvern,
PA 19355, USA

liver cells [22]. Although MageD1 was initially implicated as a substrate of Praja1 [25], this data were consistent with later studies showing that the MAGE family of proteins are binding partners and positive cofactors of RING finger ligases [26]. In light of both studies, it now appears that Praja1 likely ubiquitylates (for proteasomal destruction) an intermediary stabilizer of MageD1, possibly a DUB. Nevertheless, the interactions between the MAGE family proteins and RING finger ligases do not formally exclude the possibility that RING finger ligases ubiquitylate particular MAGE proteins, either for proteasomal destruction or non-degradative functions. Another cofactor of Praja1, UBE2D2, has been shown to interact *in vitro* and *in vivo* [24], making this a strong candidate for the functional E2 for Praja1. Proteomic study of the interaction network and substrates of Praja1 would provide better insight into this intriguing E3, and provide the basis for further experimentation. It might also help evaluate this enzyme for suitability as a target for therapeutic intervention.

Microarray approaches to the proteomic study of E3's have had great success *in vitro* identifying substrates [27–29] and interacting partners [30] of the ubiquitylation machinery. Mass spectrometric (MS) approaches have had great success *in vivo* defining the identities of ubiquitylated proteins [31, 32], the types of linkages found within the cell [33], and interacting partners of the ubiquitylation machinery [3]. A technical comparison of the advantages and disadvantages between microarray and MS aside, the *in vivo* approach (MS) excels in showing biological consequence of manipulation, while the *in vitro* approach (array) excels in showing direct consequences. Ultimately complementary, an investigator forced to choose between these two options must carefully consider which question is more important and choose accordingly.

Here, we report microarray-based identification of substrates of the human E3 Praja1. First, we demonstrate a method for optimization of the E2/E3 pairing to be tested before beginning array-based experimentation. We then identify putative substrates for this ligase using protein microarrays. Finally, we utilize Gene Ontology (GO) clustering to prioritize this list for future experimental follow up. Comparison of these results to the information about Praja1 previously available shows strong overlap, implying high quality of the data presented.

Materials and Methods

E2 Optimization

The activity of Praja1 was profiled against 18 human E2's using the E2 Profiling Kit (LifeSensors #UC102) according to manufacturer's instructions.

Ubiquitylating microarrayed substrates

Two protein microarrays (Invitrogen ProtoArray v1.0) were identically, simultaneously ubiquitylated according to manufacturer's instructions, utilizing UBE2D3 as the E2 and Praja1 as the E3 (recombinant proteins from LifeSensors.com). After washing away soluble ubiquitylation machinery, one array (PA20) was probed with ubiquitin polyclonal antibody (Sigma #U5379-1VL), capable of detecting both mono- and poly-ubiquitylation events. The other array was probed with biotinylated TUBE2 (LifeSensors #UM302), specific to polyubiquitylation. Secondary detection agents were fluorescein conjugates of anti-rabbit and streptavidin, respectively.

Array Data Acquisition and Analysis

Protein microarrays were scanned on a Typhoon Imager 9410 (GE) at 10 μm resolution using 488 nm excitation and 526 nm emission. Digitally extracted data were background corrected; technical sources of error were loess normalized globally and on print tip/location. Values were then scale normalized to print controls (AlexaAntiMouseAb ~ 33.3). Duplicate features of each printed protein were summarized by mean. Resulting values were referred to as "mean scale normalized loess normalized background corrected intensity" (MSLBICI). Features for both arrays (antibody and TUBE2 detection) were ranked by intensity (Table 1a, b). Visually confirmed ubiquitylation events and features common to both detection methods were selected for further analysis. GO clustering was then performed with the Gostat analysis package [34; <http://gostat.wehi.edu.au/>] with the goa_human database containing 33,972 genes, with Benjamini correction for multiple sampling [35] and a cutoff of 0.05 for significance.

Results

E2 Optimization for the E3 Ubiquitin Ligase Praja1

Using the E2 Profiling Kit (catalog #UC102 LifeSensors, Inc), the amount of polyubiquitin chain formation by Praja1 in concert with various E2 ubiquitin conjugating enzymes was evaluated. The assay works essentially like an ELISA, in which the polyubiquitin-specific capture reagent coating the wells of the plate pulls down from solution any polyubiquitin chain formed. A second polyubiquitin detection reagent is then added to detect and quantify the amount of chain recovered [2]. By using a consistent amount of various E2's, the preferred E2 partners of Praja1 were easily elucidated. While most E2's did not work with Praja1 the following worked well: UBE2K,

Table 1 Results from array visualized (a) with ubiquitin antibody (PA20) and (b) TUBEs (PA35)

Name	Block	Row	Clmn	Visual	Mean	Stdev	CV	GO analysis
(a) Ubiquitin antibody (PA20)								
ELAC1	44	4	11	Y	402.1	49.5	12.3	
FKB1A	47	3	3	Y	344.8	27.7	8.0	
LCP2	13	5	11	Y	341.7	54.8	16.0	
MGC11134	11	5	5	Y	333.0	34.0	10.2	
MAGEB4	18	3	7	Y	327.9	44.7	13.6	
PFKFB4	46	5	11	Y	306.2	8.8	2.9	0016301
C21orf33	14	4	9	Y	296.2	20.9	7.1	
FLJ38159	28	3	13	Y	284.3	47.4	16.7	
ABR	40	3	9	Y	277.5	31.7	11.4	
MGC4606	21	3	13	Y	272.7	22.3	8.2	
MGC17515	43	3	3	Y	267.0	34.1	12.8	
GTF2I	37	5	1	Y	264.5	22.2	8.4	0016251
CKB	15	5	11	Y	256.2	48.9	19.1	0016301, 0007420
NAGK	13	5	13	Y	253.8	12.8	5.0	0016301
GLO1	45	3	13	Y	251.1	37.3	14.9	0006916
ACY-3	5	7	1	N	246.5	26.7	10.8	
PHGDH	39	4	15	Y	242.3	29.4	12.1	0007420
PACSIN2	21	6	9	N	240.7	19.1	8.0	
STAC	39	5	1	N	238.7	4.2	1.8	
COASY	41	3	9	Y	236.7	26.4	11.1	0016301
PCTK1	13	5	3	Y	234.8	8.5	3.6	0016301
GALM	33	3	13	N	234.6	26.9	11.5	
HOMER2	36	4	5	Y	226.2	9.6	4.3	
FHL1	11	7	5	Y	223.4	62.0	27.7	
PIP5K2C	15	5	3	Y	220.2	0.7	0.3	
APEX1	4	6	5	N	216.5	24.5	11.3	
STK22C	32	3	9	Y	214.7	31.0	14.4	
TXNDC5	45	3	5	Y	214.5	92.7	43.2	0006916
TAF9	29	5	1	Y	213.0	32.8	15.4	0016251
BC008624.1	33	3	7	N	210.2	27.8	13.2	
C17orf103	32	5	9	Y	209.7	32.4	15.5	
(b) TUBEs (PA35)								
ELAC1	44	4	11	Y	1598.7	90.3	5.6	0006396
DDX54	27	3	15	Y	630.7	5.8	0.9	0006396, 0005524
MAGEB4	18	3	7	Y	587.9	46.5	7.9	
STAC	39	5	1	Y	554.2	226.5	40.9	
ABR	40	3	9	Y	402.1	96.8	24.1	
PELI2	3	6	15	N	394.7	114.3	28.9	
FKB1A	47	3	3	Y	383.4	123.1	32.1	
FGF12	34	6	5	Y	376.7	126.5	33.6	
SRSF6	7	3	3	N	372.8	22.4	6.0	
LCP2	13	5	11	Y	357.2	8.7	2.4	
CAMK1G	37	5	3	Y	331.3	82.4	24.9	0005524
TK1	23	5	9	Y	330.7	18.0	5.4	0005524
HNRNPC	28	6	9	Y	330.2	151.0	45.7	0006396

Table 1 continued

Name	Block	Row	Clmn	Visual	Mean	Stdev	CV	GO analysis
TXNDC5	45	3	5	Y	323.5	124.3	38.4	
GTF2I	37	5	1	Y	317.9	44.6	14.0	
NM_003674	12	7	11	N	304.1	395.4	130.0	
RPS6KL1	37	5	9	N	301.7	264.9	87.8	
C17orf103	32	5	9	Y	301.2	1.8	0.6	
LRG1	20	6	9	Y	282.6	11.9	4.2	
PPAP2B	19	5	1	N	282.0	142.8	50.6	
KHK	29	5	13	N	277.1	39.4	14.2	
DVL2	19	5	3	N	276.3	102.7	37.2	
CKM	31	5	3	N	275.6	164.6	59.7	
EVI5L	12	6	9	N	273.4	229.8	84.1	
PCCA	9	4	9	Y	270.9	82.3	30.4	0005524
NAGA	41	3	15	N	268.6	56.7	21.1	
MGC11134	11	5	5	Y	265.8	4.7	1.8	
ZNF193	41	6	15	N	265.1	39.5	14.9	
FLJ38159	28	3	13	Y	263.9	41.3	15.7	
TP53IP	8	3	5	N	263.4	314.6	119.4	
NAGK	13	5	13	N	262.3	182.4	69.5	0005524
TRIM41	43	7	3	N	258.8	291.2	112.5	
CYBRD1	4	5	15	N	258.5	72.3	28.0	
LOC645591	33	3	1	N	255.9	27.6	10.8	
ARAF	10	7	11	N	254.5	130.0	51.1	
METTL1	45	4	3	N	250.8	43.0	17.1	
METAP2	15	6	11	Y	242.0	29.7	12.3	
CSAG3	6	5	11	Y	241.1	112.8	46.8	
ZNF673	44	5	5	N	235.8	47.7	20.2	
PRPF3	31	4	15	N	234.2	105.9	45.2	
C3orf26	48	4	1	N	233.6	70.0	30.0	
NM_152471	43	3	3	N	228.6	119.1	52.1	
TMEM214	15	4	11	Y	221.8	33.8	15.2	
TPPP3	37	7	1	N	221.4	27.0	12.2	
ENOSF1	46	5	3	N	221.2	62.2	28.1	
MAN2C1	8	4	7	N	216.1	203.2	94.0	
ALDH1A3	40	5	1	N	213.8	148.7	69.5	
EGFR	16	7	1	N	213.6	50.4	23.6	
BC008624	33	3	7	N	213.4	95.3	44.7	
TCF19	36	6	3	N	213.3	57.4	26.9	
EPHB3	44	7	15	N	212.3	120.4	56.7	
CD2BP2	31	7	1	N	211.4	5.7	2.7	
SEPT1	10	4	11	N	210.1	110.0	52.3	
PCTK1	13	5	3	N	209.9	27.6	13.2	0005524
HMGNI	3	3	7	N	209.5	301.7	144.0	
BATF2	36	4	1	N	205.2	126.3	61.6	
FCF1	47	6	3	N	202.5	136.4	67.3	
DCAF10	9	6	15	N	201.9	555.0	274.9	
FHL1	11	7	5	N	201.6	59.5	29.5	

Table 1 continued

Name	Block	Row	Clmn	Visual	Mean	Stdev	CV	GO analysis
C21orf33	14	4	9	N	201.3	149.5	74.3	
DIRAS2	6	3	9	N	201.2	153.1	76.1	
C9orf80	46	5	5	N	199.8	11.3	5.7	

Bold emphasized proteins were common to both identification methods (antibody and TUBEs). Block, row, and column refer to physical locations of the printed proteins on ProtoArray v1.0. “Visual” refers to the presence (Y) or absence (N) of confirmed signals on the array at both spots representing the indicated protein. Mean refers to “mean scale normalized loess normalized background corrected intensity (discussed in text). Stdev refers to standard deviation, calculated from duplicate spots notwithstanding. CV is coefficient of variation. “GO analysis” lists identified categories over-represented in the dataset as assigned by the GO consortium

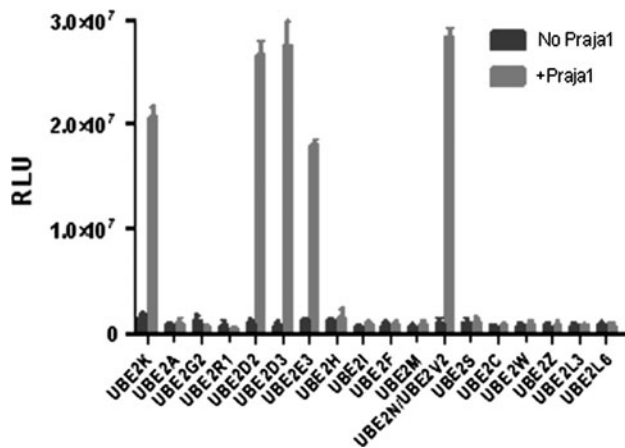


Fig. 1 E2 profiling of Praja1 revealed five different E2's were functional from among 18 tested. Based on this data, UBE2D3 was chosen for use on the arrays

UBE2D2, UBE2D3, UBE2E3, and the combination of UBE2N/UBE2V2 (Fig. 1). Consistent with published data, Praja1 worked robustly with UBE2D2 [24]. Based on slightly higher activity with UBE2D3, we chose this enzyme for use with Praja1 on subsequent arrays.

Praja1 Ubiquitylation of Microarrayed Substrates

Putative substrates of Praja1 were identified on ProtoArray v1.0 (Invitrogen), containing nearly 2000 immobilized human proteins. Ubiquitylation reactions were performed on duplicate arrays as described using UBE2D3 as the E2, Praja1 as the E3, and wild-type recombinant human ubiquitin (i.e., all seven lysines and no exogenous tags present). Array RS00009020 (“PA20”) was probed with Sigma rabbit anti-ubiquitin (#5379-1VL); array RS00009035 (“PA35”) was probed with biotinylated TUBE2 (Life-Sensors #UM302). While the antibody recognizes ubiquitin, whether it is singly attached to substrates or present in chains, TUBEs recognize only chains of ubiquitin. Figure 2 shows representative grid images from PA20 and PA35. Row 2a shows the brightest features of each array

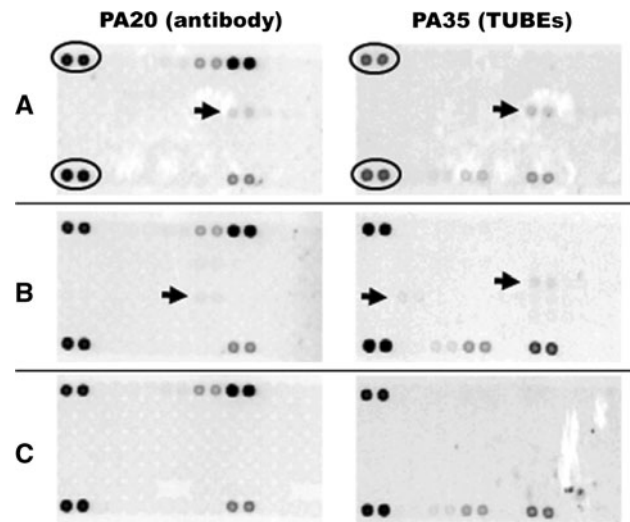


Fig. 2 Representative images of grids from both arrays representing signals of relative high intensity (row a), low intensity (b), and absent of any non-control signal (c). Positive controls used for inter-array normalization are circled, and putative Praja1 substrates are indicated by arrow

(indicated by arrows), which happen to be the same feature (grid 44, row 4, columns 11 and 12, and ELAC1). Figure 2b shows grids from both arrays in which spots were visually confirmed, but the signal intensities were extremely low. Figure 2c shows grids from both arrays in which no ubiquitylation events were observed.

Cleaning and Analyzing Data

Although not strictly necessary for highly “clean” arrays, the effect of normalizing technical sources of variation can be dramatic. Consistent with previous study [36], we found print-tip loess methods to be superior to global loess. Figure 3 shows box plots for the same subset of PA20 grids (grids 1–20) not normalized for technical sources of error (3a), global loess normalized (3b), and print-tip loess normalized (3c). Also shown are the boxplots of the complete datasets from the antibody array before (3d) and after (3e) print-tip loess normalization; data are also

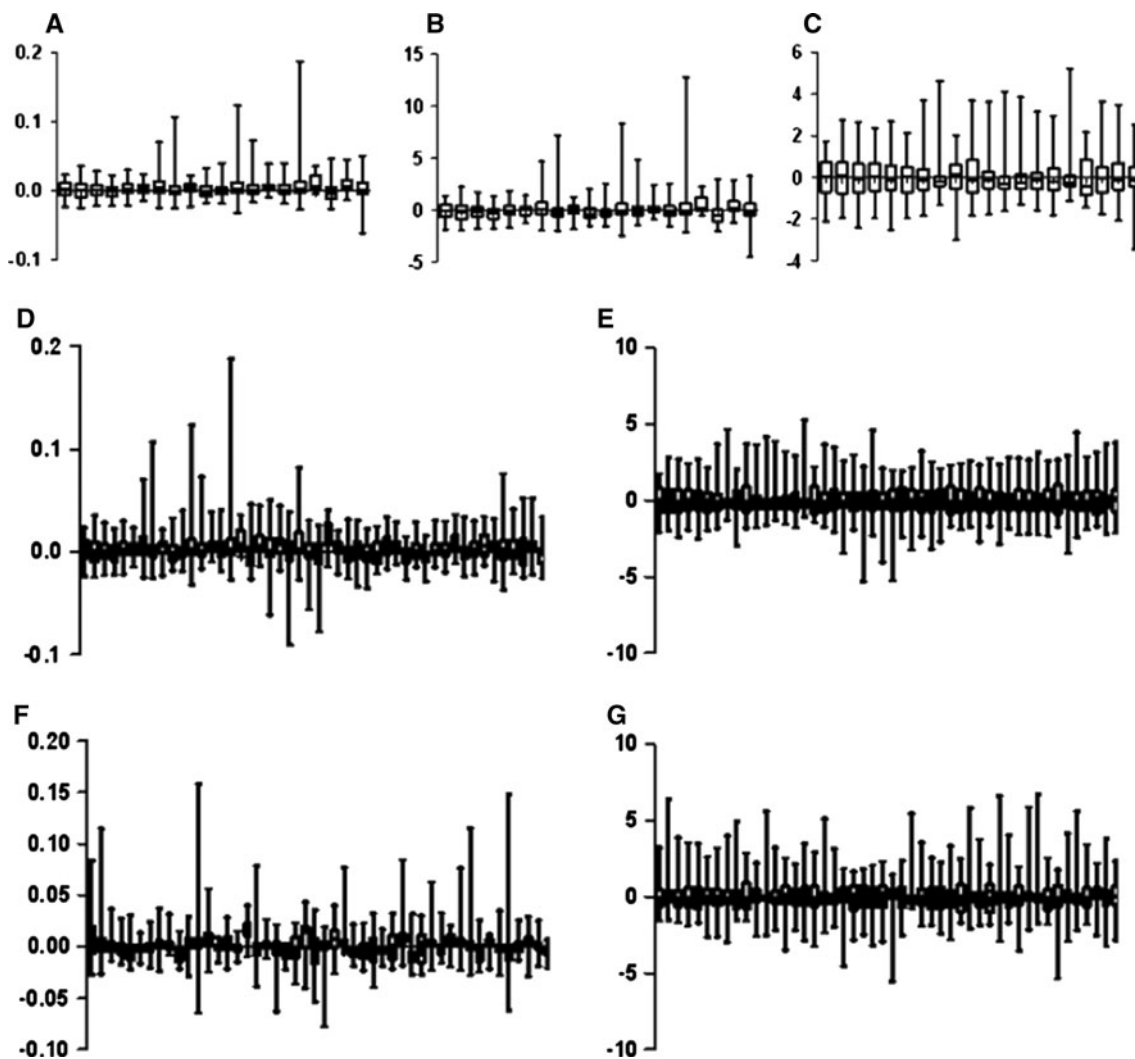


Fig. 3 Methods of normalizing technical sources of error were evaluated with a subset of the data from the antibody array (PA20). Shown are the effects of no normalization, i.e., raw data (a), global loess normalization (b), and print tip loess normalization (c). Also

shown are the complete dataset from the antibody array before (d) and after (e) print tip loess normalization; and the complete dataset from the TUBEs array (PA35) before (f) and after (g) print tip loess normalization

presented for the TUBEs array before (3f) and after (3g) normalization.

Table 1a, b shows the data obtained from both arrays with a subjective cutoff of ≥ 200 for “mean scale normalized loess normalized background corrected intensity” (reported in the Table 1a, b simply as “mean”). Each putative substrate was visually inspected for confirmation of signal above background. Removing from further consideration those features not visually confirmed, or not common to both detection methods, we find that the antibody array identified 26 putative substrates, the TUBEs array identified 25, and 14 were common to both. Figure 4 shows the Venn diagram representing these distinct but overlapping sets of substrates. From this list, we next asked if there were any subcellular locations, biological process, or molecular functions over-represented beyond what

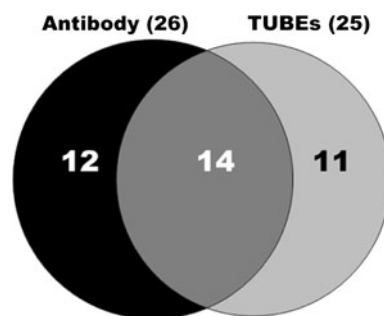


Fig. 4 Venn diagram of the putative substrates identified by each array

chance alone would predict. From the TUBEs array (PA35), 18 of the 25 putative substrates were present in the database. Six of these were annotated in ATP binding

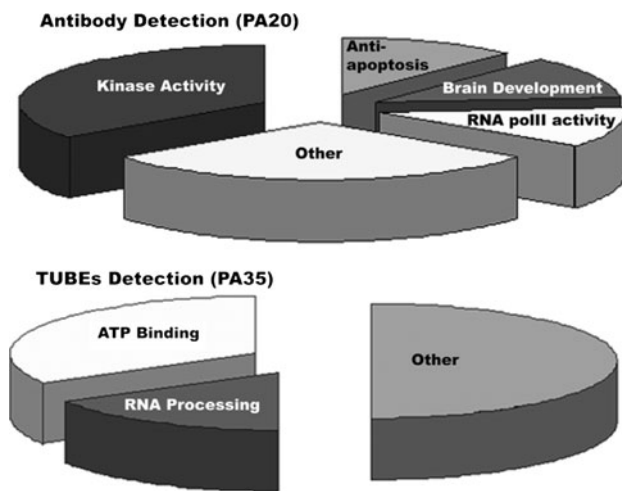


Fig. 5 GO analysis of each data set revealed unique (if partially overlapping) ontology clusters. Differences are possibly due to the TUBEs' specificity for polyubiquitylated substrates compared to antibody detection capable of recognizing both mono- and poly-ubiquitylation events

(GO:0005524, 2792 total genes in database, $P = 0.047$), and 3 were annotated in RNA processing (GO:0006396, 525 total genes in database, $P = 0.047$). From the antibody array (PA20), 17 of 26 proteins were in the database. Two of these 17 were annotated in RNA polIII transcription (GO:0016251, 41 total genes, $P = 0.011$); two were annotated in brain development (GO:0007420, 139 total genes, $P = 0.025$); two were annotated in anti-apoptosis (GO:0006916, 170 total genes, $P = 0.030$); and five were annotated in kinase activity (GO:0016301, 1697 total genes, $P = 0.016$). Figure 5 shows graphical representation of the results from this clustering.

Discussion

Traditionally, microarray-based substrate identification has utilized two arrays, one done with complete reaction mixture, the second with reaction mix lacking a critical component (most commonly the E3). The second array provides the background signal from detection reagents in the absence of ubiquitylated substrates. This facilitates statistical determination of the probability that observed signals on the complete array were “real” ubiquitylation events, represented by P value from t test under the null hypothesis that the signals do not vary. This value, along with signal intensity, is commonly used to rank the putative substrates. In this study, we chose to forego the negative control array, instead using reagents informative to the extent of chain formation. Importantly, these different primary detection reagents utilized unique secondary detection reagents. A critical step in prioritizing putative

substrates for analysis (or follow up) in this study, therefore, was selecting signals common to both arrays. In a traditional study using an array treated with incomplete reaction components, common signals indicate background. In this experimental configuration, common signal from two arrays with no shared detection reagents indicates the opposite, and provides support for a real ubiquitylation event. Our putative substrates—enriched for signals common to both arrays—were therefore ranked by signal intensity with this “hidden P value” built in.

Non-common substrates identified by each array (Table 1, Figs. 4, 5) might be non-biological noise inherent to the array experiments. Alternatively, it might reflect biological differences between polyubiquitylation and monoubiquitylation of different substrates. In support of the latter, we (unpublished results) and others [37] have observed that certain substrates are specifically monoubiquitylated *in vitro*. Because polyubiquitylation (via K48 linkage) signals proteasomal degradation, a fate shared by the majority of proteins, one would predict that detection of polyubiquitylation events would result in a more general list of substrates compared with detection of monoubiquitylation (signaling) events. Consistent with this, GO clustering of our TUBEs-detected substrates resulted in fewer categories than analysis of antibody-detected substrates (Fig. 5).

As mentioned, Praja1 is known to be highly expressed in brain, involved in memory formation, and implicated in X-linked mental retardation [21, 24]. The putative substrates representing the GO cluster “brain development” should therefore be prioritized for experimental follow up. MAGED1 interacts with MSX2, a protein elsewhere identified as a Praja1 substrate [23]. MAGED1 is a protein involved in the apoptotic response, and has also been implicated as a cofactor of Praja1 [25, 26]. The putative substrates representing “anti-apoptosis” might therefore be prioritized for independent experimental confirmation. Although MAGED1 was not present on the arrays, both array-detection methods in this study identified another MAGE family protein, MAGEB4 (Table 1a, b). Given the known involvement of MAGE proteins with RING finger ligases [26], and the open possibility that the former may be substrates of the latter (in addition to cofactors), this tandem should also be further investigated. Finally, although the GO clustering of array data qualitatively differed between the detection methods used (discussed above), involvement of Praja1 in protein translation might be suggested by the identification of putative substrates involved in “RNA PolIII activity” (antibody array) and RNA processing (TUBEs array).

Regardless of how putative substrates are identified, experimental confirmation is required. This applies to this study as well as array-based studies utilizing the traditional

negative control array. Indeed, it applies to MS-based substrate identification. Both types of proteomic studies excel in providing clues or leads. Careful experimental design, statistical analysis, and GO clustering all maximize the likelihood that putative substrates are real; but in the end microarrays cannot confirm biological relevance, and MS results cannot separate direct from indirect effects. As in most proteomic experiments, the biological insight of the researcher (based on personal and/or published data) provides additional support to certain suggested substrates. Based on that insight, many of the substrates presented for Praja1 in this study should be considered likely, if still putative.

References

- Li, W., Bengtson, M. H., Ulbrich, A., Matsuda, A., Reddy, V. A., Orth, A., et al. (2008). Genome-wide and functional annotation of human E3 ubiquitin ligases identifies MULAN, a mitochondrial E3 that regulates the organelle's dynamics and signaling. *PLoS One*, *3*, e1487.
- Marblestone, J. G., Kumar, K. G., Eddins, M. J., Leach, C. A., Sterner, D. E., Sterner, M. R., et al. (2010). Novel Approach for Characterizing Ubiquitin E3 Ligase Function. *Journal of Biomolecular Screening*, *15*, 1220–1228.
- Sowa, M. E., Bennett, E. J., Gygi, S. P., & Harper, J. W. (2009). Defining the human deubiquitinating enzyme interaction landscape. *Cell*, *138*, 389–403.
- Nijman, S. M., Luna-Vargas, M. P., Velds, A., Brummelkamp, T. R., Dirac, A. M., Sixma, T. K., et al. (2005). A genomic and functional inventory of deubiquitinating enzymes. *Cell*, *123*, 773–786.
- Todi, S. V., Winborn, B. J., Scaglione, K. M., Blount, J. R., Travis, S. M., & Paulson, H. L. (2009). Ubiquitination directly enhances activity of the deubiquitinating enzyme ataxin-3. *EMBO Journal*, *28*, 372–382.
- Chen, Z. J., & Sun, L. J. (2009). Nonproteolytic functions of ubiquitin in cell signaling. *Molecular Cell*, *33*, 275–286.
- Haglund, K., & Dikic, I. (2005). Ubiquitylation and cell signaling. *EMBO Journal*, *24*, 3353–3359.
- Grabbe, C., & Dikic, I. (2009). Functional roles of ubiquitin-like domain (ULD) and ubiquitin-binding domain (UBD) containing proteins. *Chemical Reviews*, *109*, 1481–1494.
- Weake, V. M., & Workman, J. L. (2008). Histone ubiquitination: triggering gene activity. *Molecular Cell*, *29*, 653–663.
- Sigismund, S., Polo, S., & Di Fiore, P. P. (2004). Signaling through monoubiquitination. *Current Topics in Microbiology and Immunology*, *286*, 149–185.
- Huang, T. T., & D'Andrea, A. D. (2006). Regulation of DNA repair by ubiquitylation. *Nature Reviews Molecular Cell Biology*, *7*, 323–334.
- Hochstrasser, M. (2009). Origin and function of ubiquitin-like protein conjugation. *Nature*, *458*, 422–429.
- Lee, D. H., & Goldberg, A. L. (1998). Proteasome inhibitors: valuable new tools for cell biologists. *Trends in Cell Biology*, *8*, 397–403.
- Deretic, V. (2010). Autophagy in infection. *Current Opinion in Cell Biology*, *22*, 252–262.
- Skaug, B., & Chen, Z. J. (2010). Emerging role of ISG15 in antiviral immunity. *Cell*, *143*, 187–190.
- Turnbull, E. L., Rosser, M. F., & Cyr, D. M. (2007). The role of the UPS in cystic fibrosis. *BMC Biochemistry*, *8*(Suppl1), S11–S20.
- Attaix, D., Ventadour, S., Codran, A., Béchet, D., Taillandier, D., & Combaret, L. (2005). The ubiquitin–proteasome system and skeletal muscle wasting. *Essays Biochem*, *41*, 173–186.
- Debigare, R., Cote, C. H., & Maltais, F. (2010). Ubiquitination and proteolysis in limb and respiratory muscles of patients with chronic obstructive pulmonary disease. *Proceedings of the American Thoracic Society*, *7*, 84–90.
- Rogers, N., Paine, S., Bedford, L., & Layfield, R. (2010). Review: the ubiquitin proteasome system: contributions to cell death or survival in neurodegeneration. *Neuropathology and Applied Neurobiology*, *36*, 113–124.
- Nicholson, B., Marblestone, J. G., Butt, T. R., & Mattern, M. R. (2007). Deubiquitinating enzymes as novel anticancer targets. *Future Oncology*, *3*, 191–199.
- Stork, O., Stork, S., Pape, H. C., & Obata, K. (2001). Identification of genes expressed in the amygdale during the formation of fear memory. *Learning and Memory*, *8*, 209–219.
- Mishra, L., Tully, R. E., Monga, S. P., Yu, P., Cai, T., Makalowski, W., et al. (1997). Praja1, a novel gene encoding a RING-H2 motif in mouse development. *Oncogene*, *15*, 2361–2368.
- Yoon, W. J., Cho, Y. D., Cho, K. H., Woo, K. M., Baek, J. H., Cho, J. Y., et al. (2008). The Boston-type craniosynostosis mutation MSX2 (P148H) results in enhanced susceptibility of MSX2 to ubiquitin-dependent degradation. *The Journal of Biological Chemistry*, *283*, 32751–32752.
- Yu, P., Chen, Y., Tagle, D. A., & Cai, T. (2002). PJA1, encoding a RING-H2 finger ubiquitin ligase, is a novel human X chromosome gene abundantly expressed in brain. *Genomics*, *79*, 869–874.
- Sasaki, A., Masuda, Y., Iwai, K., Ikeda, K., & Wantanabe, K. (2002). A RING finger protein Praja1 regulates Dlx5-dependent transcription through its ubiquitin ligase activity for the Dlx/Msx-interacting MAGE/Necdin family protein, Dlxin-1. *The Journal of Biological Chemistry*, *277*, 22541–22546.
- Doyle, J. M., Gao, J., Wang, J., Yang, M., & Potts, P. R. (2010). MAGE-RING protein complexes comprise a family of E3 ubiquitin ligases. *Molecular Cell*, *39*, 963–974.
- Lu, J., Lin, Y., Qian, J., Tao, S., Zhu, J., Pickart, C., et al. (2008). Functional dissection of a HECT ubiquitin E3 ligase. *Molecular and Cellular Proteomics*, *7*(1), 35–45.
- Andrews, P. S., Schneider, S., Yang, E., Michaels, M., Chen, H., Tang, J., et al. (2010). Identification of substrates of Smurf1 ubiquitin ligase activity utilizing protein microarrays. *Assay and Drug Development*, *8*, 471–487.
- Gupta, R., Kus, B., Fladd, C., Wasmuth, J., Tonikian, R., Sidhu, S., et al. (2007). Ubiquitination screen using protein microarrays for comprehensive identification of Rsp5 substrates in yeast. *Molecular Systems Biology*, *3*, 116.
- Balut, C. M., Loch, C. M., Gao, Y., Devor, D. Role of ubiquitination and Usp8 (UBPY)-dependent deubiquitination in the endocytosis and lysosomal targeting of plasma membrane KCa3.1 (submitted).
- Shi, Y., Chan, D. W., Jung, S. Y., Malovannaya, A., Wang, Y., Qin, J. (2010). A dataset of human endogenous protein ubiquitination sites. *Molecular and Cellular Proteomics*. doi:10.1074/mcp.M110.002089.
- Meierhofer, D., Wang, X., Huang, L., & Kaiser, P. (2008). Quantitative analysis of global ubiquitination in HeLa cells by mass spectrometry. *Journal of Proteome Research*, *7*, 4566–4576.
- Xu, P., Duong, D., Seyfried, N., Cheng, D., Xie, Y., Robert, J., et al. (2009). Quantitative proteomics reveals the function of unconventional ubiquitin chains in proteasomal degradation. *Cell*, *137*, 133–145.

34. Beissbarth, T., & Speed, T. P. (2004). GOstat: Find statistically overrepresented gene ontologies within a group of genes. *Bioinformatics*, *20*, 1464–1465.
35. Benjamini, V., & Hochberg, V. (1995). Controlling the false discovery rate: a practical and powerful approach to multiple testing. *Journal of the Royal Statistical Society B*, *57*, 289–300.
36. Loch, C. M., Ramirez, A. B., Liu, Y., Sather, C. L., Delrow, J. J., Scholler, N., et al. (2007). Use of high density antibody arrays to validate and discover cancer serum biomarkers. *Molecular Oncology*, *1*, 313–320.
37. Wada, K., & Kamitani, T. (2006). UnpEL/USP4 is ubiquitinated by Ro52 and deubiquitinated by itself. *Biochemical and Biophysical Research Communications*, *342*, 253–258.